frontiers in
EARTH SCIENCE

ORIGINAL RESEARCH ARTICLE
published: 24 February 2015
doi: 10.3389/feart.2015.00007

The impact of climate change on landslides in southeastern of high-latitude permafrost regions of China

Wei Shan*, Zhaoguang Hu, Ying Guo, Chengcheng Zhang, Chuanjiao Wang, Hua Jiang, Yao Liu and Jitao Xiao

Institute of Cold Regions Science and Engineering, Northeast Forestry University, Harbin, China

Edited by:
Davide Tiranti, Regional Agency for Environmental Protection of Piemonte, Italy

Reviewed by:
Dranreb Earl Juanico, Technological Institute of the Philippines, Philippines
Fabio Matano, National Research Council, Italy
Claudia Meisina, University of Pavia, Italy

****Correspondence:***
Wei Shan, Institute of Cold Regions Science and Engineering, Northeast Forestry University, Harbin 150040, China
e-mail: shanwei456@163.com

Climate warming leads to permafrost degradation and permafrost melting phase transition, resulting in an increasing number of landslides. This study uses the road segments and road area at the intersection between Bei'an-Heihe Highway and the northwest section of the Lesser Khingan Range in north China as the study area. By means of geological survey combined with meteorological data, we analyzed the impact of climate change on landslide movement in the permafrost zone. Over a 60 year period, the average annual temperature of the study area has increased by 3.2°C, and permafrost degradation is severe. Loose soil on the hillside surface provides appropriate conditions for the infiltration of atmospheric precipitation and snowmelt, and seepage from thawing permafrost. As it infiltrates downwards, water is blocked by the underlying permafrost or dense soil, and infiltrates along this barrier layer toward lower positions, forming a potential sliding zone. The representative Landslide in the study area was examined in detail. Displacement monitoring points were set up on the surface of the landslide mass, and at the trailing edge of the landslide mass. The data collected were used to investigate the relationship between landslide movement and pore water pressure at the tailing edge as well as the ground temperature. The results show that the landslide movement process changes with the season, showing a notable annual cyclical characteristic and seasonal activity. Landslide movement is characterized by low angles and intermittence. The time of slide occurrence and the slip rate show a corresponding relationship with the pore water pressure at the tailing edge of the landslide mass. The seepage of water from thawing into the landslide mass will influence the pore water pressure at the tailing edge of the landslide mass, and is the main cause of landslide movement.

Keywords: climate change, high-latitude permafrost, permafrost degeneration, landslide movement, pore water pressure

INTRODUCTION

In northeast China, the area north of 47°N contains widespread permafrost. This is China's only high-latitude permafrost region, and is also China's second largest permafrost region (Guo et al., 1981; Zhou et al., 1996; Sun et al., 2007). In recent years, due to the effects of climate change, the southern boundary of China's northeast high-latitude permafrost region gradually moved northward. Permafrost near the southern boundary shows discontinuous island-like distribution and accelerated degradation (Jin et al., 2000; He et al., 2009a; Wei et al., 2010).

Climate is the long-term average state of atmospheric physical characteristics. Climate change refers to the change in the mean state of climate over time. In the last century, the average global surface temperature has been continuously increasing, which shows a consistent warming trend worldwide. The rate of warming during the past 50 years is almost twice that of the past 100 years [IPCC (Intergovernmental Panel on Climate Change), 2007]. Since the early 1980s, in most of the permafrost regions in the world, the temperature has increased. In some regions in northern Alaska, the observed temperature increase has reached 3°C, in the northern European region and Russia, the increase has reached 2°C. In the latter region, during the 1975–2005 period substantial reduction in the thickness and range of the permafrost layer was observed (IPCC, 2013). Climate change and its impact are an important research issue receiving extensive global attention.

Numerous studies have shown that the climate change in China exhibits the same trend as the global climate change (Ding et al., 2006). In the last 54 years, the rate of temperature increase in China was about 0.25°C/10a, far higher than the global or hemispheric average rate of warming. Northeast China is one of the areas showing the most significant warming and permafrost degradation in the country (Shi et al., 2014).

Forest and accumulated snow have a very important influence on the temperature change and the thawing process of the underlying seasonal frozen ground and permafrost (Chang et al., 2011). In the Great and Lesser Khingan Ranges of northeast China and the Outer Baikal region of Russia, temperature shifts caused by snow, vegetation, water, topography, atmospheric inversion, and other local factors are substantial, forming the "Khingan–Baikal

type" that is permafrost distinctly from polar and high-altitude permafrost distribution (Zhou and Guo, 1982; Chang et al., 2013). Affected by the occurrence conditions, the process and form of high-latitude permafrost degradation in northeast China are also different from that of polar and high-altitude permafrost (Jin et al., 2009).

In recent years, landslide incidents triggered by climate change and extreme weather have increased (Blunden and Arndt, 2011), and have gradually received attention from national governments and relevant international academic organizations (Eu-Fp7, 2008; ICL, 2014). In particular, landslides in cold areas are becoming a hot issue in landslide research [ICL (International Consortium on Landslides), 2012; Guo et al., 2013].

Landslides are a natural geological phenomenon in mountainous areas. Their mechanism and evolution are closely related to the geological conditions and environmental factors, and are controlled not only by geological forces, lithologic structure, and other crustal internal factors; but also by topography, land cover, precipitation, changes in human activities, and environmental conditions. The spatial and temporal distribution of landslides has characteristics of uncertainty, sporadic nature, continuation, and irreversibility. Landslides are the result of geological and environmental changes and in turn also drastically change the geological environment (Shan et al., 2014b). Scientists have applied different methods in order to analyze the relationship between climate change and landslide mechanisms and evolution in cold areas (Shan et al., 2014a). The impact of landslides induced by glacier and permafrost degradation in cold regions; on the topography, geological environment, water resources, and biodiversity has been examined; and the role of climate, a main factor influencing the landslide movement, in the evolution of landslides in cold areas has been discussed (Fischer et al., 2013; Haeberli, 2013; Kliem et al., 2013; Starnberger et al., 2013; Ballantyne et al., 2014; Grab and Linde, 2014; Nussbaumer et al., 2014). However, due to lack of monitoring data, the majority of these studies were large-scale (Stoffel et al., 2014). Currently, there has been no report on the mechanisms, movement characteristics, and patterns of landslides induced by the combined effect of permafrost thawing and extreme weather events due to climate change and geological conditions.

In the present study, the road area where the Bei'an to Heihe Highway crosses the northwest section of the Lesser Khingan Range is used as the study area. We performed a geological survey, an engineering survey, and field measurements which were plotted on the topographic map of the landslide area and a relevant geological cross section. Using the meteorological data of Sunwu County (30 km from the study area), which was released by the China Meteorological Data Sharing Service System (http://cdc.cma.gov.cn/home.do), we analyzed the impact of climate change on permafrost thaw, geological environment, and landslide mechanisms in the study area. Using Landslide K178 + 530 in the landslide area as an example, we used monitoring data of point displacement on the landslide mass, ground temperature at the trailing edge, and pore water pressure to perform a comprehensive analysis of the impact of climate change on the pore water pressure at the measuring points and the landslide movement process.

BACKGROUND

China's Bei'an-Heihe Highway intersects the northwest section of the Lesser Khingan Range at the junction between Sunwu County and the Aihui District. The study area lies between east longitude 127°17′31″-127°21′24″ and north latitude 49°30′57″-49°41′50″ (**Figure 1**). The area is located on the southern fringe of China's high-latitude permafrost region and has typical periglacial landforms. The island-like permafrost in this region is the result of to residual paleo-glacial deposition and is currently in the degradation stage. The geological conditions are extremely unstable.

TOPOGRAPHY AND GEOLOGICAL STRUCTURE

The study area is located in the northwest section of the Lesser Khingan Range. It has a hilly landscape with undulating terrain. The slope of the ground is generally 10–20°, and the upper part of the slopes are relatively steep, about 25–30°, but locally can be up to 40°. The area can be further divided into the valley bottomland and hills. The altitude of the entire area ranges from 210–330 m.

The geological structure of the study area belongs to the Khingan-Haixi fold belt. From the bottom up, the stratigraphy is composed by Cretaceous mudstone, Tertiary pebbly sandstone, silty mudstone, and powdery sandstone. From the late Tertiary to the early Quaternary, the Lesser Khingan Range experienced block uplift. Due to long-term erosion and leveling, loose sediments on the summit and the slope of the hills have gradually thinned, and the thickness of the current residual layer is generally only 1–2 m. The loose deposits accumulate mainly in the basin and valley areas between mountains, with a thickness of about 10 m. The soil is mainly composed of clayey silt, mild clay, and gravelly sand, and the surface is covered with a relatively thick layer of grass peat and turf. The surface vegetation is that of grassland and woodland, and there are inverted trees in the woodlands. **Figure 2** shows the geological map of the landside road area of the study area plotted from the field survey conducted in June 2010.

CLIMATE CONDITIONS

The study area is located in the transition zone between the north part of the middle-temperate zone and the cold-temperate zone. The area is affected by alternating influences of high and low pressures from inland and the sea as well as by monsoons. Overall the climate is characterized by long, dry and cold winters and short, hot and humid summers. In other words, it belongs to the continental monsoon climate zone.

The average annual temperature in this area ranges −2–1°C, with an extreme maximum of 38.6°C, and an extreme minimum of −48.1°C. The annual average wind speed is 2.7–4.0 m/s. The average annual precipitation is 530–552 mm, with a maximum of 800 mm. Precipitation is mostly concentrated in the summer, from July to September, accounting for 61–67% of the total annual precipitation. The first snow fall is typically in mid-October, and the final snow fall is often in late March or early April of the following year. The maximum annual evaporation is greater than 1000 mm, whereas the minimum is 850 mm. The average annual sunshine is 2500 h, with a maximum of 2800 h and a minimum of 2200 h. The total amount of annual radiation averages 1148 kcal/cm^2, with a maximum of 1229 kcal/cm^2, and a minimum of 1039 kcal/cm^2.

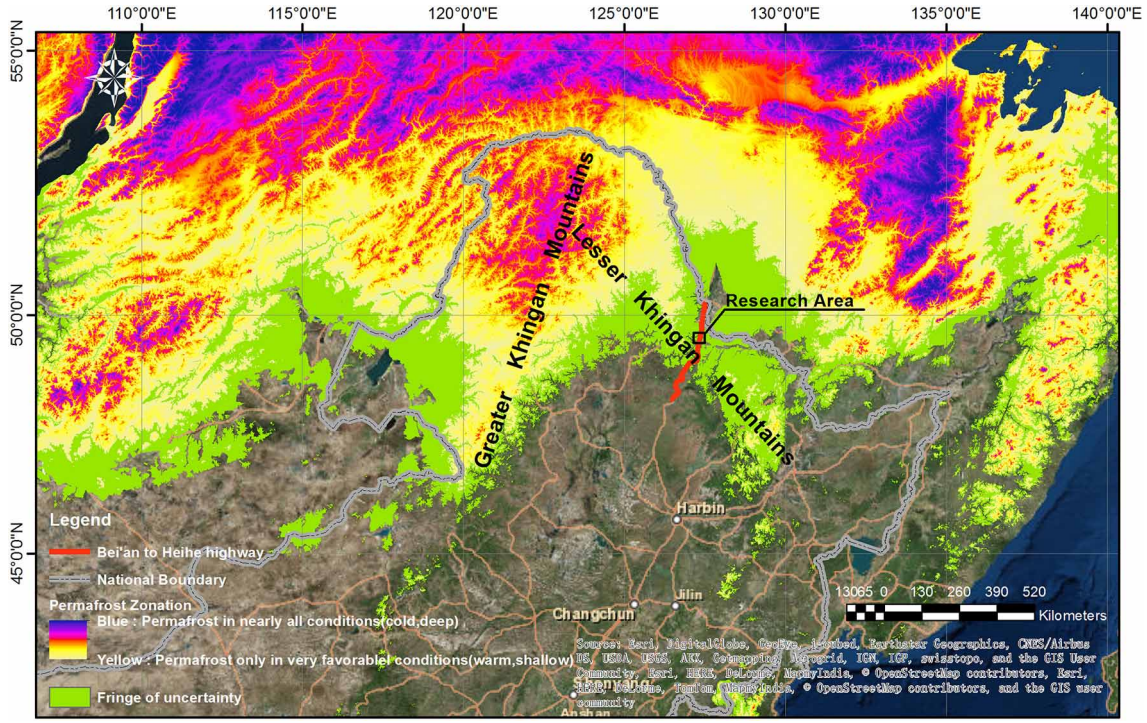

FIGURE 1 | High-latitude permafrost distribution in Northeast China (data from Zurich University, Switzerland), and the location of study area.

PERMAFROST DISTRIBUTION

The climate in Northeast China is controlled by the Siberia—Mongolia high-pressure control. The inversion layer is widely distributed in this region and has an important impact on the development process and regional distribution of permafrost. Meanwhile, the northeast region of China is China's main forest distribution area, where the ecological environments of wetlands, grasslands, and forests coexist with permafrost mutually restraining and influencing each other. Forests, bushes, mosses, and other ground covers reduce solar radiation, hindering the increase of air and ground temperatures. The low-lying river terraces, valleys, wetlands, and shady slopes provide good conditions for the development and preservation of island-like permafrost and slow permafrost degradation.

The seasonal ground freezing in the study area reaches maximum depth at the end of May, and the observed maximum depth is 2.26–2.67 m. In the mountains, the maximum seasonal freezing depth exceeds this value. April to September is the thawing period of seasonal frost; in dry areas all the seasonal frost thaws in early July, whereas in swamped thick peat and humus zones, seasonal frosts do not completely thaw until the end of October. On shady slopes and in valley areas, island-like permafrost is distributed.

Because there is no long-term meteorological data for the study area obtained from field measurements, meteorological data from Sunwu County (30 km from the study area), published by the China Meteorological Data Sharing Service System, was used for the analysis of climate change. **Figure 3** plots the monthly average temperatures, soil temperatures in 40 cm depth, atmospheric precipitations, and maximum permafrost thicknesses from 1971–2000 using meteorological data of Sunwu County.

CLIMATE CHANGE OF THE STUDY AREA

Affected by global climate change, the study area has become one of the regions in northeast China with the largest temperature increase in the past 50 years. Meteorological data of Sunwu County show that in the past 60 years, among all climate indicators, change in temperature was the most significant. **Figure 4** shows the annual average maximum temperatures, average temperatures, average minimum temperatures, and average precipitation from 1954–2013 using meteorological data of Sunwu County. By applying linear regression, we found that, over the 60 year period from 1954 to 2013, the annual average temperature in the study area increased by 3.2°C; the average annual maximum temperature increased by 1.5°C, or 21.99%; the average annual minimum temperature increased by 5.2°C, or 69.04%; and the average annual precipitation decreased by 4.85 cm, or 8.93%. The increase in the average annual minimum temperature was 3.45 times that of the average annual maximum temperature.

CLIMATE CHANGE AND LANDSLIDES

Climate change leads to permafrost degradation in the study area, and human engineering projects further accelerate the process of permafrost degradation (He et al., 2009b). In 1999, a survey conducted for constructing the secondary road from Bei'an to Heihe showed that there were 17 permafrost road segments along the entire road length (Wang et al., 2001; Zhang et al., 2001).

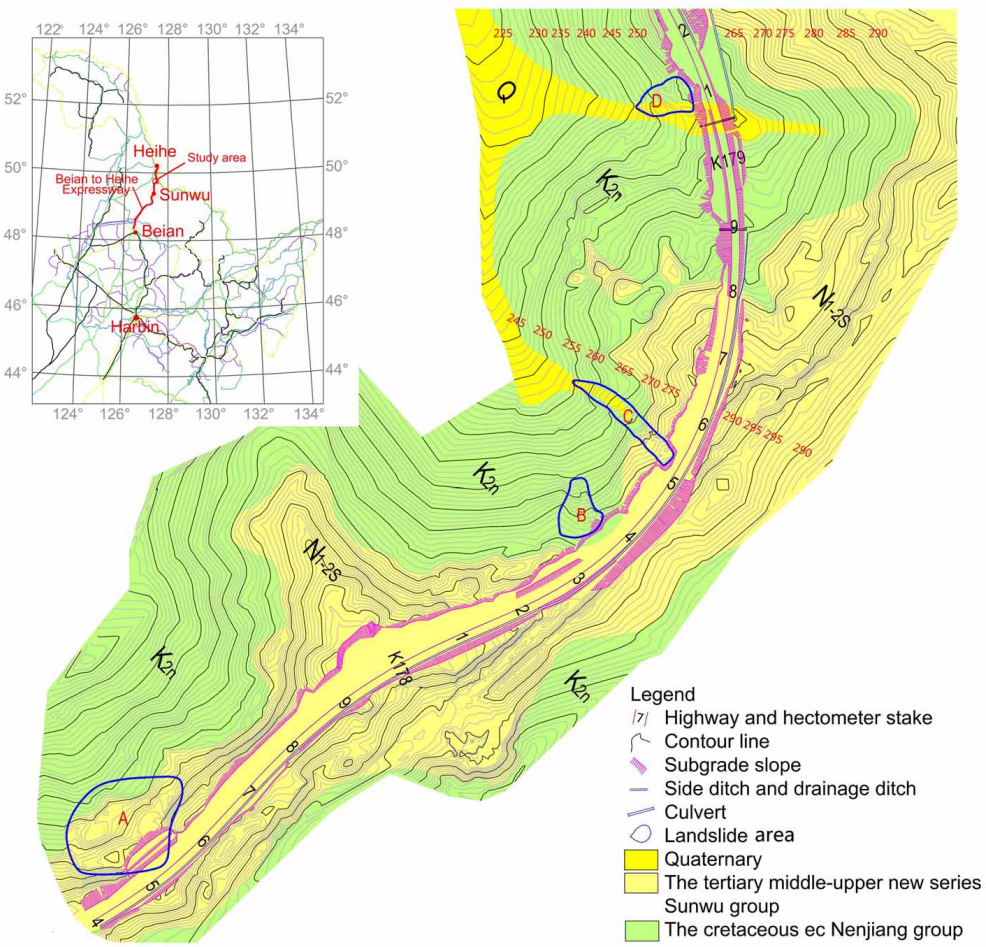

FIGURE 2 | Geological map of K177+400-K179+200 section of Bei'an-Heihe Highway.

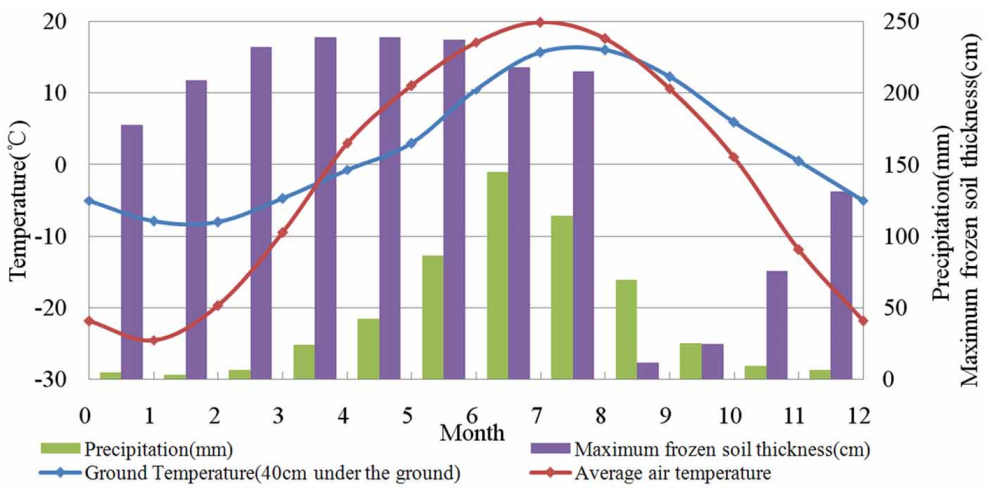

FIGURE 3 | Monthly average temperature/soil temperature in 40 cm depth/permafrost thickness/precipitation in Sunwu County (1971–2000, Data: China Meteorological Data Sharing Service System).

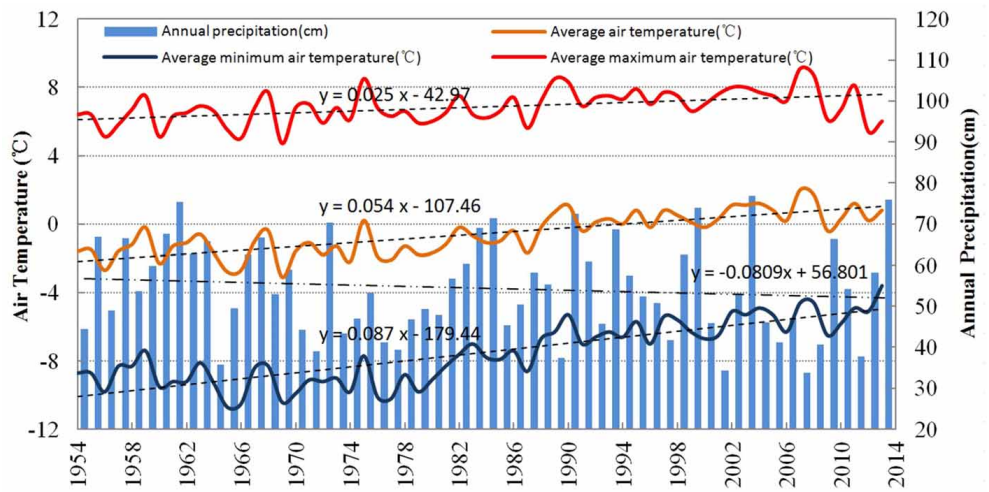

FIGURE 4 | Annual average maximum temperatures, average temperatures, average minimum temperatures and average precipitation in Sunwu County (1954–2013).

Yet in 2009, a survey conducted right before the construction of the Bei'an-Heihe Highway showed that there were only six permafrost road segments remaining; the other 11 segments had been completely degraded.

During the thawing of permafrost, the phase change of water has a severe impact on the mechanical properties of the soil (Wang et al., 2014b). Permafrost degradation causes a lot of geological engineering problems in the construction of roads. The construction of the Bei'an-Heihe secondary road started in 1999, and in August 2000 on the K176 + 900 − 178 + 200 section a landslide was induced by thawing of permafrost in the roadbed. This caused instability of the entire roadbed in this section, which had to be completely abandoned. The road was then redirected toward the left along the ridge, as shown in **Figure 5A**.

The survey conducted before the 2009 project of widening the Bei'an-Heihe road and constructing the Bei'an-Heihe Highway also showed that, in the K177 + 400 - K179 + 200 section, within 10 m of the left of the roadbed there were four landslides with a volume of over 20000 m^3, as illustrated in **Figure 2**. In addition, a number of landslides were found within 3 km of this road area (**Figure 6**), thus forming the landslide group at the intersection where the Bei'an-Heihe Highway crosses the northwest section of the Lesser Khingan Range. When compared with the permafrost distribution map obtained from the Enhanced Thematic Mapper (ETM+) imaging data collected from satellite Landsat7 in 2009 (**Figure 7**) (Wang et al., 2014a), it can be seen that the locations of the landslides fit the permafrost distribution very well. Thus, we deduced that these landslides were induced by the thawing of permafrost.

MONITORING OF LANDSLIDE MOVEMENT

In June 2010, on the basis of geological survey and topographic measurements of the study area, comprehensive examination and dynamic monitoring of the slip movement were performed on a representative landslide that may threaten the roadbed in order to investigate the impact of permafrost thaw on landslide movement.

Landslide K178 + 530 on the Bei'an-Heihe Highway (**Figure 2C**) is one of the landslides that is closest to the roadbed and has the fastest slip rate. Because survey and monitoring data prior to 2009 are not available, the time of the initial slip could not be determined. From the satellite photo taken on June 15, 2004, it can be seen that at that time the straight-line distance between the leading edge and the tailing edge of the landslide mass was 101.26 m (**Figure 5B**). The satellite photo taken on September 12, 2010 showed that the straight-line distance between the leading and tailing edges of the landslide mass had increased to 145.05 m (**Figure 5C**). Over this 6 year period, the leading edge of the landslide moved forward 43.79 m, whereas the position of the trailing edge basically did not change.

Figure 8 shows the distribution of the drillings, the geophysical measurement lines and points for monitoring displacement, ground temperature, and pore water pressure for Landslide K178 + 530. The points A, B, C, D, E, and F in the figure denote the positions of the drilling, and lines G and H denote the high-density resistivity measurement line and the ground-penetrating radar (GPR) measurement line, respectively. During the drilling in holes E and F, permafrost was found at a depth 2.2 m below the ground surface, and the permafrost thicknesses at points E and F were 3.7 m and 2.4 m, respectively. The area of permafrost distribution in **Figure 8** is inferred according to **Figure 7**.

Through drilling, GPR, and high-density resistivity prospecting; the profiles of Landslide K178 + 530 in cross section H along the sliding direction and in cross section G perpendicular to the slide direction were obtained (**Figures 9**, **10**).

In boreholes A and B shown in **Figure 8**, plastic displacement measurement piles with a length of 400 cm and an above-ground height of 30 cm were buried; the top of the pile was used to monitor the slope displacement of the landslide mass at points A and B. C served as the monitoring point of the ground temperature; in the borehole, thermistor soil temperature sensors were set up at

FIGURE 5 | Satellite photos of K176 + 500 - K179 + 900 section of Bei'an-Heihe Highway (Google earth). (A) Landslide in K178+530 section (in 2000). **(B)** Satellite photos of K178 + 530 (2004.6). **(C)** Satellite photos of K178+530 (2010.9).

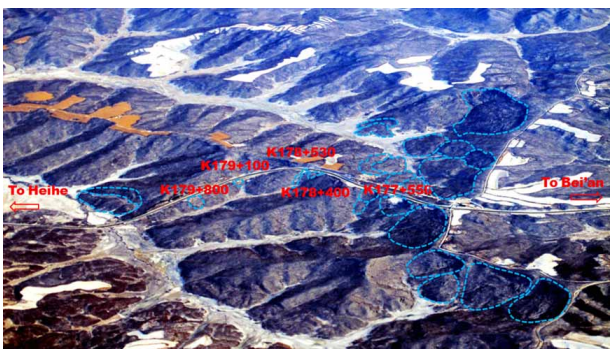

FIGURE 6 | Full view of K175 + 500 - K180 + 200 section of Bei'an-Heihe Highway (Blue line is the boundary of the landslides, the orange area is corn field).

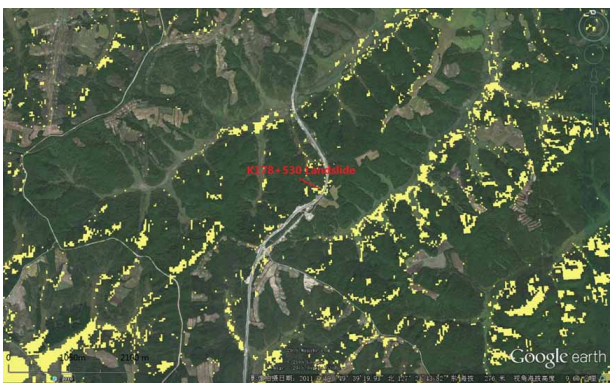

FIGURE 7 | Permafrost distribution map in K176 + 500 - K180 + 000 section of Bei'an-Heihe Highway.

every 0.5 m from 0.5 to 2.5 m below the ground surface. D served as the monitoring point of pore water pressure; in the borehole, steel-wire soil pore water pressure sensors were set up at 3.8, 9.4, 19.4, and 23.7 m below the ground surface. Regular monitoring of relevant parameters started in July 2010.

The real-time dynamic deformation monitoring system, a Real Time Kinematic -Global Positioning System (RTK-GPS), was used to monitor the displacements of the measuring points on the landslide surface. From July 2010 to August 2014, point A slid horizontally by 69.03 m, and its elevation dropped by 7.95 m; point B slid horizontally by 113.97 m, and its elevation dropped by 17.37 m. Based on these values, it can be deduced that the angle between the slope and the horizontal plane decreased from 8.07° to 6.02°. Points A′ and B′ in **Figures 8**, **9** show the positions of points A and B, respectively, in August 2014 after sliding.

Figure 11 shows the average daily ground temperatures and atmospheric precipitations over time at point C on Landslide K178 + 530 at depths of 0.5 and 2.0 m. The ground temperature data is on-site monitoring data; the average daily atmospheric temperatures and precipitations are meteorological data collected at Sunwu County weather station.

To facilitate data analysis, the soil freeze period was defined as the period from the time when the thermistor sensor at 0.5 m below ground surface detected temperature below 0°C in the autumn to the time when the thermistor sensor at 2.0 m below ground surface detected temperature changing from below to above 0°C in the spring. This period is displayed in light blue

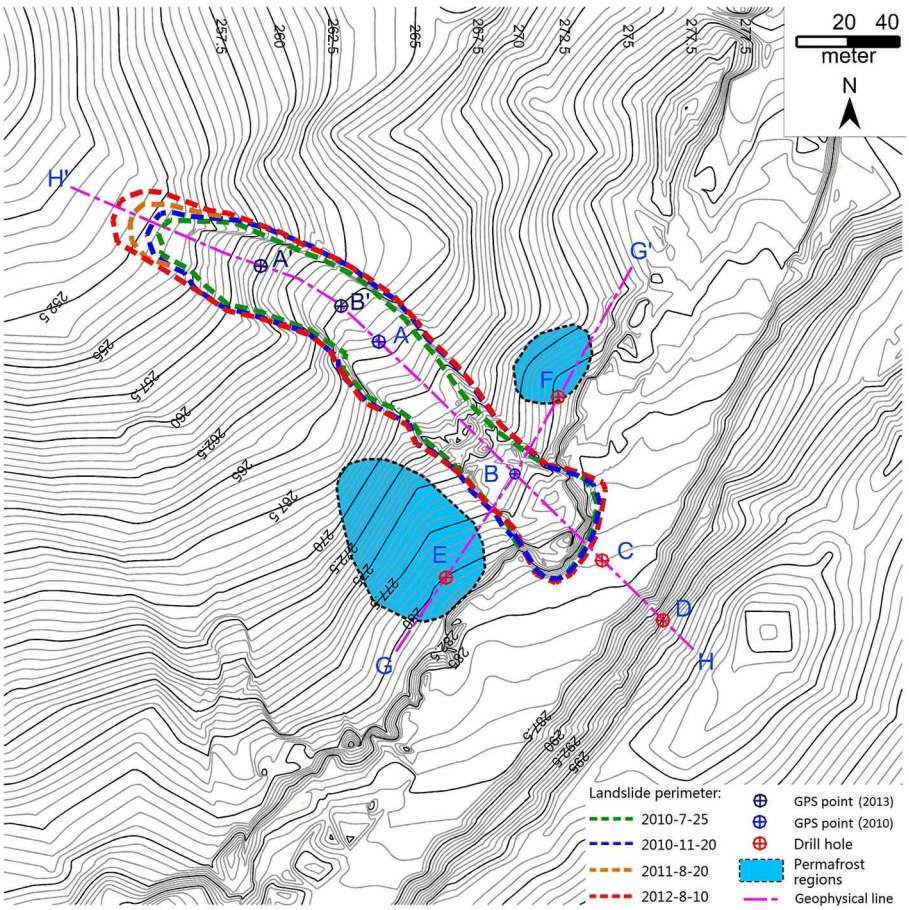

FIGURE 8 | Distribution of the drillings, the geophysical measurement lines and points for monitoring displacement, ground temperature, and pore water pressure in Landslide K178 + 530.

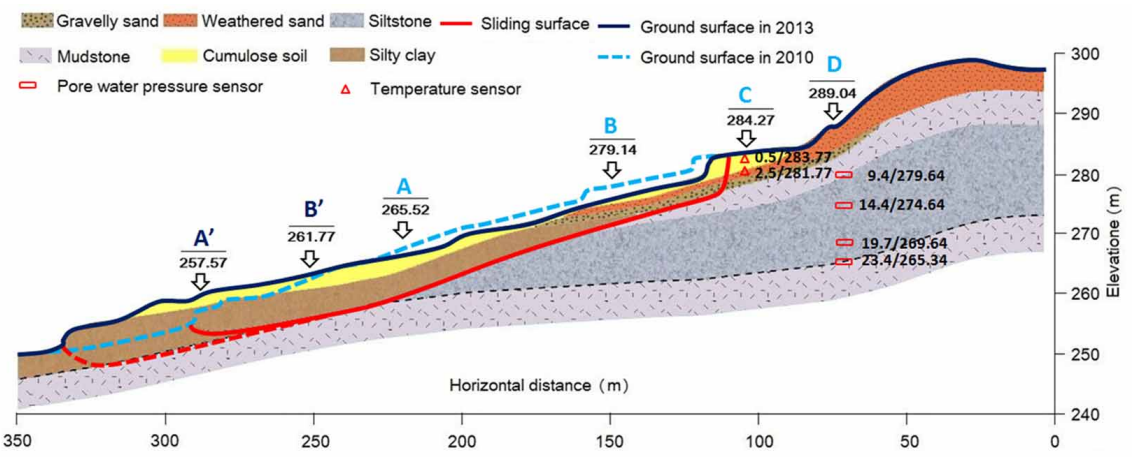

FIGURE 9 | The profiles of Landslide K178 + 530 along the sliding direction.

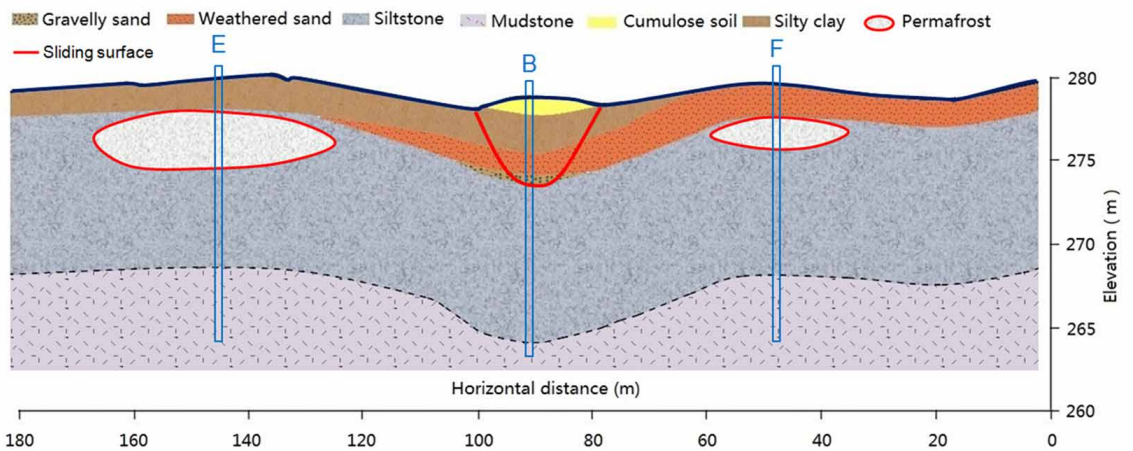

FIGURE 10 | The profiles of Landslide K178 + 530 perpendicular to the slide direction.

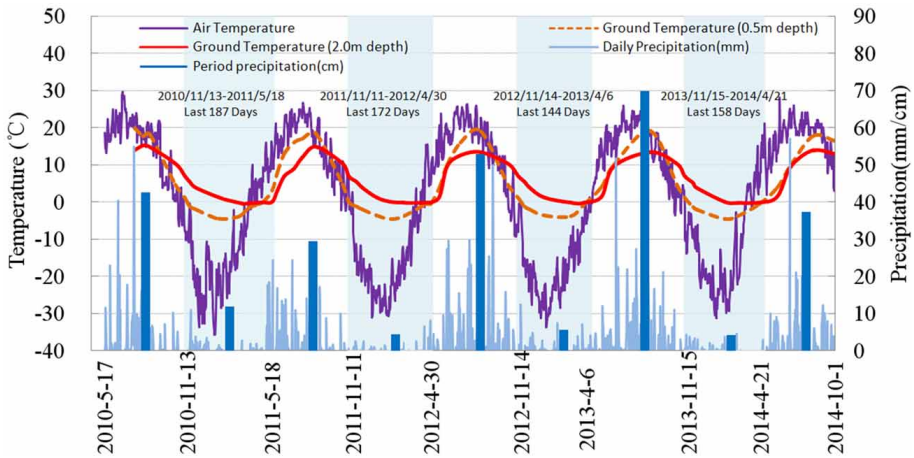

FIGURE 11 | Daily average air temperature/precipitation/soil temperature in the depth of 50 cm, 200 cm in K178 + 530 section of Bei'an-Heihe Highway.

in **Figure 11**. The sums of atmospheric precipitation over the soil freeze period and non-freeze period were calculated, and are denoted by the dark blue bars in **Figure 11**. During the soil freeze period, atmospheric precipitation and snowmelt water are blocked by the seasonal frozen soil layer and cannot normally infiltrate downward to deep soil.

Figure 12 shows the pore water pressure measured at point D, 19.4 m below the ground surface. At point D at the time of drilling, water was first observed at a depth of 3.8 m below the ground surface, but the stable water level measured during the monitoring period ranged from 15.8 to 16.6 m. Soil at 3.8 and 9.4 m below the ground surface was found to be unsaturated during the monitoring period. Readings from the pore water pressure sensor placed at 23.7 m below the ground surface were unstable during the late stage of monitoring, and thus data collected from the sensor placed at 19.4 m below the ground surface are used to represent pore water pressure at point D.

Figure 13 illustrates changes in the displacement rates at point A and point B on the landslide mass, and in pore water pressure at point D over time. To obtain the displacement rate, displacement data collected using the RTK-GPS real-time dynamic deformation monitoring system were divided by the monitoring interval.

RESULTS, ANALYSIS, AND DISCUSSION

The permafrost distribution determined by the present study is consistent with previous investigations (Wang et al., 2014a, 2015). In the current study, meteorological data of Sunwu County, 30 km south of the study area, was analyzed to examine the climate change in the study area. The causes of landslide in the study area were evaluated preliminarily by means of permafrost distribution, topography, geological survey of the study area, and investigation on the specific case of roadbed instability occurring in section K176 + 900 − 178 + 200 on a Bei'an-Heihe secondary road in August 2000.

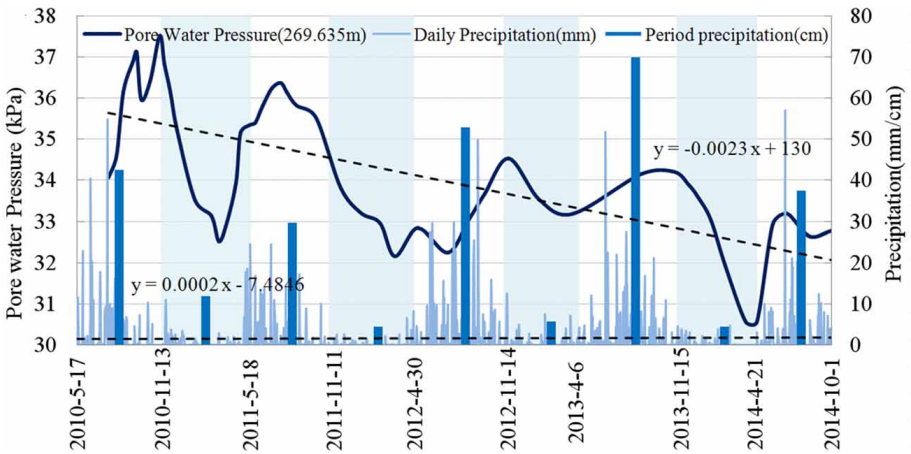

FIGURE 12 | Daily precipitation and pore water pressure in the depth of 19.4 cm of D point in K178 + 530 section of Bei'an-Heihe Highway.

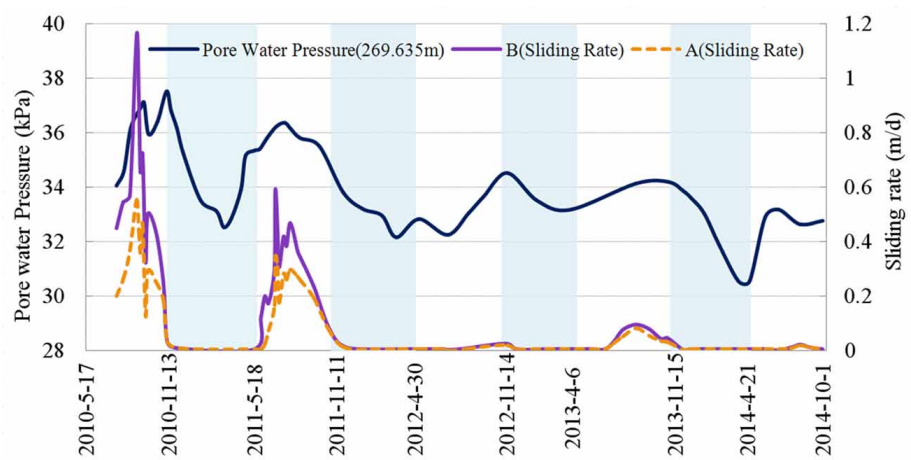

FIGURE 13 | Horizontal displacement rates at point A and point B on the landslide mass and pore water pressure at point D (19.4 m depth) in K178 + 530 section of Bei'an-Heihe Highway.

The Sunwu County meteorological data show that, over the 60 year period from 1954 to 2013, the variation in atmospheric precipitation was 8.93%, and that this had little long-term effect on the thermal state of the soil in the study area. As shown in **Figure 4**, the increase in the average annual minimum temperature was substantially higher than the increase in the average annual maximum temperature. This suggests that the main cause of the temperature rising was not the increase in the amount of direct radiation, but rather the decrease in the heat demand of the soil from the atmosphere and the increase in the ability of the soil to radiate heat into the atmosphere (Chen et al., 2006). The difference in the amplitude of temperature increase between the average annual maximum temperature and the average annual minimum temperature was caused by the latent heat of permafrost thaw. The fact that the amplitude of temperature increase in the average annual maximum temperature and in the average annual minimum temperature differed by 47.05% over a 60 year period demonstrates that the permafrost in the study area is decreasing in amount, going through rapid degeneration.

In **Figure 7**, permafrost is not found in section K176 + 900 – 178 + 200 (where overall roadbed instability occurred) of the previous Bei'an-Heihe secondary road. This is because the ground temperature data used to plot **Figure 7** are the ETM+ data collected by satellite Landsat7 in 2009, whereas the roadbed instability occurred in August 2000. After 9 years, the permafrost in this road section had degraded entirely. In **Figure 7**, along the road direction on both sides of point B, which is to the right of the road section K178 + 530, there are permafrost distributions. Yet in **Figure 8E**, in borehole B no permafrost was found; in addition, in the exploration of line G using a high-density resistivity method and GPR, no data abnormality was detected below point B within 15 m along line G, demonstrating that there was no permafrost distribution. This may be because permafrost in this location was at a stage of severe degradation; and although the soil temperature was low, the phase transition of soil moisture

had already taken place and had transitioned to warm permafrost or melting permafrost. It may also be related to the resolution of the Landsat7 satellite ETM+ data.

From **Figure 11**, it can be seen that each ear the initial soil freezing in the study area occurred in a relatively concentrated time period, between 11 November and 15 November. But for the same measurement point, the time needed for seasonal frost to complete thawing varied rather largely from year to year. This may be related to the amount of autumn precipitation and winter snowfall in the previous year, as well as the thermal condition of soil water near the maximum seasonal frost depth, but needs to be further investigated.

As shown in **Figure 12**, at point D the pore water pressure started to rise in the spring of each year, reached the peak value in the summer, and then fell, thus showing annual periodic changes. But on an interannual time scale, pore water pressure showed an overall downward trend. This change was not correlated with atmospheric precipitation. Linear analysis showed that, over the monitoring period, the atmospheric precipitation in the study area increased by 0.318 mm, whereas the pore water pressure at point D decreased by 3.675 kPa. In other words, the groundwater level dropped by 36.75 cm, and the amount of groundwater reduction was 1155 times the increase in the atmospheric precipitation over the same period.

From **Figure 13**, it can be seen that the slip rates at measurement points A and B on the landslide mass correspond well to pore water pressure at point D. During the monitoring period, with the snowmelt and thawing of seasonal frost each spring, the pore water pressure in the hillside soil gradually increased, and the landslide mass started to slip. During the concentrated rainfall in the summer, the pore water pressure reached the peak for the year, and the slip rate of the landslide reached the peak value simultaneously. Along with the landslide movement, the soil pore water pressure gradually decreased, and the slope sliding gradually stagnated. The landslide movement had notable characteristics of annual periodicity and seasonal activity.

Figures 9, **13** reveal that changes in the slip rates of points A and B on the landslide mass were consistent. Over the monitoring period, the displacement of point B was 1.65 times that of point A. We deduced that the movement of point A might be occurring due to the force coming from the rear part of the landslide mass. From **Figure 13**, it can also be seen that the annual maximum pore water pressures at point D from 2010 to 2014 were 37.52, 36.37, 34.53, 34.14, and 33.19 kPa, respectively, declining year by year, and the decline in amplitude was relatively large in 2012. The maximum slip rates of point B from 2010 to 2014 were 115.7, 59, 2.55, 9.63, and 2.2 cm/d, respectively. Rapid sliding mainly occurred in 2010 and the summer of 2011. The slip rate decreased year by year, and the largest decline occurred in 2012. But in the summer of 2013, there was a slight increase in the slip rate. The reason behind these phenomena might be related to the fact that at points E and F (**Figure 8**), which are located outside the lateral edge of the slope at point B, permafrost thawed and supplemented water to the landslide mass. In addition, this might be related to the amount of summer precipitation. As shown in **Figure 12**, in 2013 the summer atmospheric precipitation reached the highest value over the entire monitoring period, 672 mm; this was 14.33 mm higher than the second highest summer precipitation (occurring in 2012) and 1.46 times the mean summer atmospheric precipitation over the monitoring period. We thus concluded that, in the monitoring period, the slip rate of Landslide K178 + 530 was mainly controlled by pore water pressure at the tailing edge of the landslide mass, and meanwhile it was also affected by the amount of summer precipitation in the study area. The pore water pressure at the tailing edge of the landslide mass was related to the thawing of permafrost at the lateral edge of the slope. As permafrost thawed year by year, its volume was reduced, which gradually reduced the pore water pressure at the tailing edge of the slope. As a result, the slip rate of the landslide mass was gradually reduced year by year.

CONCLUSION

In this study, we performed a comprehensive analysis of climate change data in the study area and data on the displacement, ground temperature, and pore water pressure at measurement points on Landslide K178 + 530 in Bei'an-Heihe Highway, and from this analysis we obtained the following main conclusions.

First, affected by the global climate change, the northwest section of the Lesser Khingan Range located at the southern boundary of the high-latitude permafrost region in northeast China experiences temperature increase, and the amplitude of the increase in average annual minimum temperature is 3.45 times that in average annual maximum temperature. Permafrost degradation is severe. Permafrost degradation will lead to further temperature rise in this region, and the northward movement of the southern boundary of the permafrost region will also accelerate.

Second, permafrost thaw causes the number of landslides in the northwest section of China's Lesser Khingan Range to increase, which results in topographical changes in this region. Human construction activity accelerates the thawing of permafrost.

Third, water seepage from thawing permafrost and infiltration of concentrated summer precipitation together increase the local moisture content in hillside soil. This is the main cause of landslides in the northwest section of the Lesser Khingan Range in China.

Fourth, in the northwest section of China's Lesser Khingan Range, landslide movement begins in the summer season with concentrated precipitation each year, and gradually stops in the autumn when the soil freezes. The landslide movement clearly has characteristics of seasonal and annual periodicity.

Fifth, the slip rate and movement process of landslides in the northwest section of China's Lesser Khingan Range are controlled by the thawing process of permafrost on and near the landslide mass. As the permafrost thaws year by year, its volume is reduced, and its ability to supplement water to the landslide mass is also reduced. This causes the slip rate of the landslides to decrease year by year until it reaches zero, and then the landslides tend to become stable.

ACKNOWLEDGMENTS

We thank the Science and Technology Project of the Chinese Ministry of Transport (2011318223630) and the International

Landslide Research Program (IPL-167) for funding support. We are also grateful to an anonymous referee who helped improve the manuscript.

REFERENCES

Ballantyne, C. K., Sandeman, G. F., Stone, J. O., and Wilson, P. (2014). Rock-slope failure following Late Pleistocene deglaciation on tectonically stable mountainous terrain. *Q. Sci. Rev.* 86, 144–157. doi: 10.1016/j.quascirev.2013.12.021

Blunden, J., and Arndt, D. S. (2011). *State of the Climate in 2011*. American Meteorological Society. Available online at: http://www.ncdc.noaa.gov/bams-state-of-the-climate/

Chang, X. L., Jin, H. J., and He, R. X. (2013). Review of permafrost monitoring in the northern Da Hinggan Mountains, Northeast China. *J. Glaciol. Geocryol.* 35, 93–100. doi: 10.7522/j.issn.1000-0240.2013.0011

Chang, X. L., Jin, H. J., Yu, S. P., Sun, H. B., He, R. X., Luo, D. L., et al. (2011). Influence of vegetation on frozen ground temperatures the forested area in the Da Xing'anling Mountains, Northeastern China. *Acta Ecol. Sin.* 31, 5138–5147.

Chen, J., Sheng, Y., and Cheng, G. D. (2006).Discussion on protection measures of permafrost under the action of engineering from the point of earth surface energy balance equation in Qinghai Tibetan Plateau. *J. Glaciol. Geocryol.* 28, 223–228.

Ding, Y. H., Ren, G. Y., and Shi, G. (2006). National assessment report of climate change (I): climate change in China and its future trend. *Adv. Clim. Change Res.* 2, 3–8.

Eu-Fp7. (2008). *ACQWA: Assessing Climate Impacts on the Quantity and Quality of Water A Large Integrating Project Under EU Framework Programme 7 (FP7), A Summary for Policymakers*. Available online at: www.acqwa.ch

Fischer, L., Hugge, C., Kääb, A., and Haeberli, W. (2013). Slope failures and erosion rates on a glacierized high-mountain face under climatic changes Earth Surf. *Process. Landforms* 38, 836–846. doi: 10.1002/esp.3355

Grab, S. W., and Linde, J. H. (2014). Mapping exposure to snow in a developing African context: implications for human and livestock vulnerability in Lesotho. *Nat. Haz.* 71, 1537–1560. doi: 10.1007/s11069-013-0964-8

Guo, D. X., Wang, S. L., Lu, G., Dai, J. B., and Li, E. Y. (1981). Regionalization of permafrost in the Da and XiaoXing'anling Mountains in northeastern China. *J. Glaciol. Geocryol.* 3, 1–9.

Guo, Y., Canuti, P., Strom, A., Hideaki, M., and Shan, W. (2013). The First Meeting of ICL landslides in cold regions network, harbin, 2012. *Landslides* 10, 99–102. doi: 10.1007/s10346-012-0369-x

Haeberli, W. (2013). Mountain permafrost - research frontiers and a special long-term challenge. *Cold Reg. Sci. Technol.* 96, 71–76. doi: 10.1016/j.coldregions.2013.02.004

He, R. X., Jin, H. J., Chang, X. L., Lv, L. Z., Yu, S. P., Yang, S. Z., et al. (2009b). Degradation of permafrost in the northern part of northeastern China:present state and causal analysis. *J. Glaciol. Geocryol.* 31, 829–834.

He, R. X., Jin, H. J., Lv, L. Z., Yu, S. P., Chang, X. L., Yang, S. Z., et al. (2009a). Recent changes of permafrost and cold regions environments in the northern part of northeastern China. *J. Glaciol. Geocryol.* 31, 525–531.

ICL. (2014). "*The 2014 Beijing Declaration Landslide Risk Mitigation: Toward a Safer Geo-environment.*" Available online at: http://iplhq.org/category/home/

ICL (International Consortium on Landslides). (2012). "*International Consortium on Landslides Strategic Plan 2012-2021- To create a safer geo-environment.*" Available online at: http://iplhq.org/category/home/

IPCC. (2013). *Summary for Policymakers. Working Group I Contribution to the IPCC Fifth Assessment Report Climate Change 2013: The Physical Science Basis*. Cambridge, UK: Cambridge University Press.

IPCC (Intergovernmental Panel on Climate Change). (2007). *Summary for Policymakers. Climate Change 2007: The Physical Science Basis. Contribution of Working Group I to the Fourth Assessment Report of the Intergovernmental Panel on Climate Change*. Cambridge: Cambridge University Press.

Jin, H. J., Li, S. X., Wang, S. L., and Zhao, L. (2000). Impacts of climatic change on permafrost and cold regions environments in China. *Acta Geogr. Sin.* 55, 161–173.

Jin, H. J., Wang, S. L., and Lv, L. Z. (2009). Features of permafrost degradation in Hinggan Mountains, northeastern China. *Sci. Geogr. Sin.* 2, 223–228.

Kliem, P., Buylaert, J. P., Hahn, A., Mayrd, C., Murray, A. S., Ohlendorf, C., et al. (2013). Magnitude, geomorphologic response and climate links of lake level oscillations at Laguna Potrok Aike, Patagonian steppe. *Q. Sci. Rev.* 71, 131–146. doi: 10.1016/j.quascirev.2012.08.023

Nussbaumer, S., Schaub, Y., Huggel, C., and Nat, A. W. (2014). Risk estimation for future glacier lake outburst floods based on local land-use changes. *Hazard. Earth Sys. Sci.* 14, 1611–1624. doi: 10.5194/nhess-14-1611-2014

Shan, W., Guo, Y., Wang, F., Marui, H., and Strom, A. (2014a). *Landslides in Cold Regions in the Context of Climate Change*. New York, NY: Springer, Environmental Science and Engineering. doi: 10.1007/978-3-319-00867-7

Shan, W., Guo, Y., Zhang, C., Hu, Z., Jiang, H., and Wang, C. (2014b). Climate-change impacts on embankments and slope stability in permafrost regions of bei'an-heihe highway. *Landslide Sci. Safer Geoenviron.* 1, 155–160. doi: 10.1007/978-3-319-04999-1_18

Shi, P. J., Sun, S., and Wang, M. (2014). Climate change regionalization in China (1961-2010). *Sci. China: Earth Sci.* 44, 2294–2306. doi: 10.1007/s11430-014-4889-1

Starnberger, R., Drescher, S. R., Reitner, J. M., Rodnight, H., Reimer, P. J., and Spötl, C. (2013). Late Pleistocene climate change and landscape dynamics in the Eastern Alps: the inner-alpine Unterangerberg record (Austria). *Q. Sci. Rev.* 68, 17–42. doi: 10.1016/j.quascirev.2013.02.008

Stoffel, M., Tiranti, D., and Huggel, C. (2014). Climate change impacts on mass movements - case studies from the European Alps. *Sci. Total Environ.* 2014, 1255–1266. doi: 10.1016/j.scitotenv.2014.02.102

Sun, G. Y., Yu, S. P., and Wang, H. X. (2007). Causes south borderline and subareas of permafrost in Da Hinggan Mountains and Xiao Hinggan Mountains. *Sci. Geogr. Sin.* 27, 68–74.

Wang, B., Sheng, Y., and Liu, J. P. (2001). Distribution and degradation of permafrost in Xiao Hinggan Mountains along the Heihe -Dalian Highway. *J. Glaciol. Geocryol.* 23, 302–306.

Wang, C., Shan, W., Guo, Y., Hu, Z., and Jiang, H. (2014a). Permafrost distribution study based on landsat ETM+ imagery of the northwest section of the Lesser Khingan Range. *Landslide Sci. Safer Geoenviron.* 3, 529–534. doi: 10.1007/978-3-319-04996-0_81

Wang, C., Shan, W., Guo, Y., Hu, Z., and Jiang, H. (2015). Permafrost distribution research based on remote sensing technology in northwest section of lesser Khingan Range in China. *Eng. Geol. Soc. Territory* 1, 285–290. doi: 10.1007/978-3-319-09300-0_53

Wang, S. H., Qi, J. L., Yin, Z. Y., Zhang, J. M., and Ma, W. (2014b). A simple rheological element based creep model for frozen soils. *Cold Reg. Sci. Technol.* 106, 47–54. doi: 10.1016/j.coldregions.2014.06.007

Wei, Z., Jin, H. J., and Zhang, J. M. (2010). Prediction of permafrost changes in Northeastern China under a changing climate. *Sci. China Earth Sci.* 41, 74–84. doi: 10.1007/s11430-010-4109-6

Zhang, Y., Wu, Q. B., and Liu, J. P. (2001). Distribution characteristics of the permafrost in the section from Heihe to Bei' an in the Xiao Hinggan Mountains. *J. Glaciol. Geocryol.* 23, 312–317.

Zhou, Y. W., and Guo, D. X. (1982). Principal characteristics of permafrost in China. *J. Glaciol. Geocryol.* 4, 1–19.

Zhou, Y. W., Wang, Y. X., Gao, X. W., and Yue, H. S. (1996). Ground temperature, permafrost distribution and climate warming in northeastern China. *J. Glaclol. Gecryol.* 18, 139–147.

Conflict of Interest Statement: The authors declare that the research was conducted in the absence of any commercial or financial relationships that could be construed as a potential conflict of interest.

Received: 16 October 2014; accepted: 08 February 2015; published online: 24 February 2015.

Citation: Shan W, Hu Z, Guo Y, Zhang C, Wang C, Jiang H, Liu Y and Xiao J (2015) The impact of climate change on landslides in southeastern of high-latitude permafrost regions of China. Front. Earth Sci. ***3****:7. doi: 10.3389/feart.2015.00007*

This article was submitted to Quaternary Science, Geomorphology and Paleoenvironment, a section of the journal Frontiers in Earth Science.